A New Method for Optimizing the Size of Axial FOV in TOF-PEM to Improve Performance of the Scanner

Delband Roshani (MSc)[1], Saeed Setayeshi (PhD)[1]*

[1]Department of Energy Engineering and Physics, Amirkabir University of Technology, Tehran, Iran

ABSTRACT

Background: Positron Emission Mammography (PEM) is a nuclear medicine imaging tool, playing a significant role in the diagnosis of patients with breast cancer. These days, many research has been done in order to improve the performance of this system.

Objective: This study aims to propose a new method for optimizing the size of axial Field of View (FOV) in PEMs and improving the performance of the systems.

Material and Methods: In this analytical study, a conventional Inveon PET is simulated using GATE in order to validate the simulation. For this simulation, the mean relative difference is 2.91%, showing the precision and correction of simulation and consequently it is benchmarked. In the next step, for design of the new optimized detector, several validated simulations are performed in order to find the best geometry.

Results: The best result is obtained with the axial FOV of 101.7 mm. It has $1.6 \times 1.6 \times 15$ mm^3 lutetium yttrium orthosilicate (LYSO) crystals. The detector consists of 6 block rings with 30 detector blocks in each ring. In this paper, the performance of the scanner is improved and the geometry is optimized. Sensitivity and scatter fraction of the designed scanner are 4.65% and 21.2%, respectively, also noise equivalent count rate (NECR) is 105.442 kcps.

Conclusion: The results showed 1 up to 3% improvement in the sensitivity of this new detector compared with different PEMs.

Introduction

Positron Emission Mammography (PEM) is a highly accurate way to diagnose breast cancer in patients. When positrons collide with electrons, annihilation occurs and the arrival time of two 511 keV positron annihilation photons should be measured. Therefore, the location of positron annihilation can be constrained. This procedure has known as time of flight Positron Emission Tomography (TOF-PET) [1-5].

There are different parameters which are momentous in PET systems. One of them is sensitivity because higher sensitivity makes less dose of radiotracer for the patients. Sensitivity is defined as the number of counts per unit time detected by the detectors for each unit of activity present in a source. There are several items, affecting the sensitivity

*Corresponding author:
Saeed Setayeshi
Department of Energy Engineering and Physics, Amirkabir University of Technology, Tehran, Iran
E-mail:
Setayesh@aut.ac.ir

such as detection efficiency of 511 keV photons, detector spatial angular coverage, timing window and energy window. Other important parameters are noise equivalent count rate (NECR) and scatter fraction that NCER is equal to the square of the signal to noise ratio (SNR). Therefore, enhancing this parameter increases the quality of images and when the scatter fraction is low, the performance of PET is better, and high quality in images would be obtained [6-7].

The geometry of the detectors has an essential effect on the parameters of PET systems and various PETs have different geometries. The first PEM had two planar detectors to compress the breast to obtain better results in images like Clear-PEM that has lutetium yttrium orthosilicate (LYSO) crystals with the size of $2\times2\times20$ mm^3 in the 64×48 crystal arrays [8]. Also, some PEMs have detectors with the capability of rotating like PEM Flex Naviscan, which every detector module had LYSO crystals with the size of $2\times2\times13$ mm^3 [9]. Furthermore, ring detector was used in some cases such as MAMMI, designed with LYSO crystals with the size of $40\times40\times10$ mm^3 and twelve modules in each ring [10].

To investigate PET, NU 4—2008 Standard was used, designed for the performance evaluation of small animal PET scanners and used for the breast tissue. In this study, Inveon PET, which is one the best commercial tomography, has been simulated by *GEANT 4 Application for Tomographic Emission (GATE)* to validate simulations (the mean relative difference was 2.91%). Inveon PET had good sensitivity, 7.5% for energy window of 250-750 keV and timing window of 4ns (with LSO crystals). Peak of NECR was 538 kcps at 131400 kBq, and this peak was obtained for the rat phantom. Scatter fraction was 0.22 for this system. Therefore, it has good parameters among other PEMs [11-13].

Material and Methods

In this analytical study, a new designed PEM was simulated in GATE V7.2 open source. It consists of 6 rings in axial Field of View (FOV), each ring has 30 modules that every module has 10×10 crystal arrays. The size of a crystal is $1.6\times1.6\times15$ mm^3 with a pitch of 1.67 mm. A model of the designed PEM is shown in Figure 1.

At first, geometry of the scanner must be defined and then for some cases, phantom should be added (for example, this part is not necessary for calculation of the sensitivity). Setting up the physics processes must be defined. The digitizer for each particle's physical observables, including energy, position, and time of detection, should be added. Next part is defining the source. The advantage of GATE is that desired format of the output can be selected, and after these steps, the acquisition could be started [14-15].

In the crystals, LYSO was used with excellent traits for detecting 511 keV gammas in PEM. For the physics part, photoelectric effect, Rayleigh, Compton, bremsstrahlung, multiple scattering, ionization and positron annihilation were added. Also, setting up the digitizer which has several parts (like an adder and readout) was added in GATE.
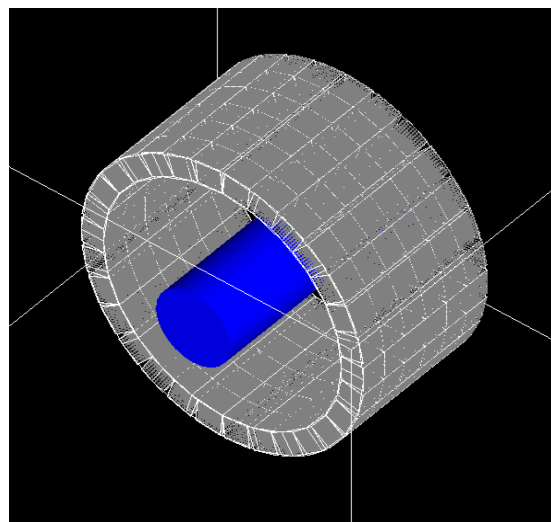

Figure 1: Schematic drawing of the designed detector of time of flight Positron Emission Mammography (TOF-PEM) in GEANT 4 Application for Tomographic Emission (GATE).

In order to benchmark the simulation, the Inveon PET that has high sensitivity and resolution has been simulated and consists of 64 detector blocks in 4 rings. Each block has 20×20 crystal arrays using lutetium orthosilicate (LSO) as material. Each crystal has 10.0 mm length. The crystal pitch is 1.59 mm in both axial and transaxial. The detector ring diameter is 16.1 cm while the axial FOV is 12.7 cm [16].

Results

Performance Evaluation
Sensitivity

Sensitivity is normally expressed in counts per second per microcurie (or megabecquerel) (cps/μCi or cps/kBq). For calculating this parameter, ^{22}Na point source (0.3 mm diameter) was used. The sensitivity was calculated for 2 energy windows, 350-650 keV and 250-750 keV and for timing windows of 2.8 and 3.4 ns. In Table 1, the experimental and simulated data of Inveon PET were shown.

For designed detector, sensitivity was calculated with LYSO crystals, timing window of 6 ns and energy window of 250-750 keV. This plot was obtained by putting a point source in different places in the direction of the axial FOV, as seen in Figure 2.

In this design, different parameters were considered. Indeed, beside sensitivity, the length of the axial FOV and the number of used crystals should be considered. Therefore, two parameters were defined for calculating optimized geometry. In Equations 1 and 2,

Table 1: Absolute sensitivity values for a ^{22}Na point source with lutetium orthosilicate (LSO) crystals and different energy windows (350–650 keV and 250–750 keV) and two coincidence windows (2.8 and 3.4 ns).

Energy Window (keV)	Coincidence Window	Experimental Inveon PET (%) [13]	Simulated Inveon PET (%)	Relative Difference (%)
350-650	2.8	5.72	5.80	1.3
350-650	3.4	5.75	6.04	5.04
250-750	2.8	7.40	7.18	2.9
250-750	3.4	7.40	7.58	2.4

PET: Positron Emission Tomography

these parameters were expressed.

$$S_{AFOV} = \frac{100 \times sensitivity\,(\%)}{length\,of\,axial\,FOV\,(cm)} \qquad (1)$$

$$S_{NC} = \frac{10000 \times sensitivity\,(\%)}{number\,of\,crystals} \qquad (2)$$

S_{AFOV} is the sensitivity regarding length of the axial FOV as shown in Equation. 1 and S_{NC} is the sensitivity considering the number of crystals in Equation. 2. Based on these equations, the higher sensitivity and the shorter length of the axial FOV lead to the better parameters.

Indeed, optimized geometry should be calculated. Therefore, the plots of these two equations were shown for different axial FOVs and the best geometry was obtained for 10.17 cm
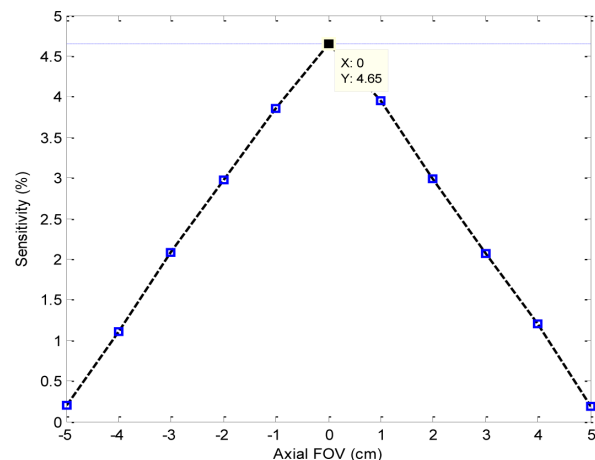

Figure 2: Sensitivity (%) of the scanner for timing window of 6 ns and energy window of 250-750 keV.

as axial FOV. It was led to 6 repetitions during the Z axial.

In Figure 3, these two parameters were plotted, showing the peak of axial FOV in the 10.17 cm.

NECR

Comparing performance of count rate between different tomographs or one scanner, working in different situations is hard. Therefore, one parameter, regarding these features needs to be defined. Noise Equivalent Count Rate (NECR) is proportional to the signal-to-noise (SNR) in images, thus, it is a good parameter to compare the performances of different PET scanners. Some parameters cause different NECR such as the geometry of the detector, the size of the object and activity of the radiotracers.

Equation 3 was used for calculating the NECR.

$$NECR = \frac{(TC)^2}{TC + SC + RC} \qquad (3)$$

In this equation, TC is the true coincidence, SC is the scatter coincidence and RC is the random coincidence [17]. For obtaining Figure 4 that is the plot of NECR with different activity concentrations, energy window of 350-650 keV with timing window of 4 ns was used.

For calculation of this parameter, it was necessary to regard a phantom with the same size as the breast. Based on NU 4—2008 Standards, a rat phantom that is a cylinder with 150

mm long, a 50 mm diameter and a hole was used that has a density of 0.96 g/cm³. Also, for this, a line source with Fludeoxyglucose (F-FDG or FDG), should be put [14].

Scatter Fraction

Another parameter is the scatter fraction that was shown in Equation 4.

$$Scatter\ Fraction = \frac{RC}{TC + RC} \qquad (4)$$

As stated, the RC and TC are random and true coincidences [18].

Based on Equation 4, when the scatter fraction is low, the performance of PET is better, and high quality in images would be obtained. Also, scatter fraction is plotted based on the activity concentrations (kBq/ml), as shown in Figure 5 that scatter fraction is 0.212 in the peak of NECR.

In Table 2, comparison of parameters for new design detector and other common detectors were provided.

Discussion

Improving the performance of the scanner in PEMs is significant to improve parameters of the system which results in less dose for the patients as well as better quality in images. In this study, the simulation of Inveon PET was done to prove the accuracy of the simulations, and the difference error was 2.91% based on Table 1; thus, it was confirmed that the simulations were valid. In the following, a new
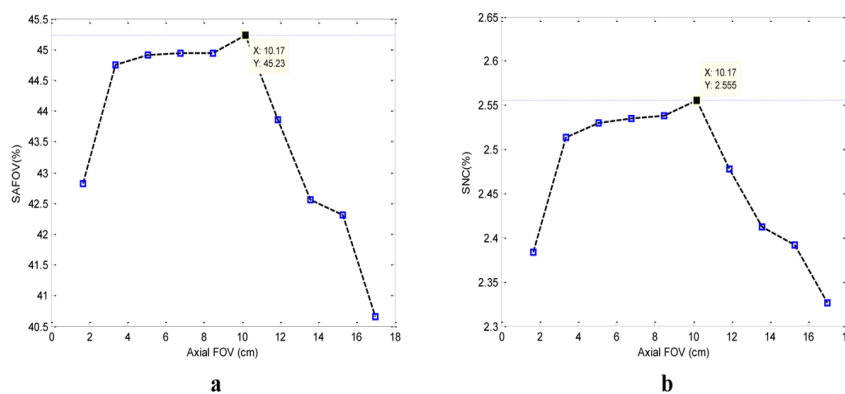

Figure 3: a) Sensitivity regarding length of axial Field of View (FOV) (S_{AFOV}) in different axial FOVs and b) sensitivity regarding the number of used crystals (S_{NC}) in different axial FOVs.
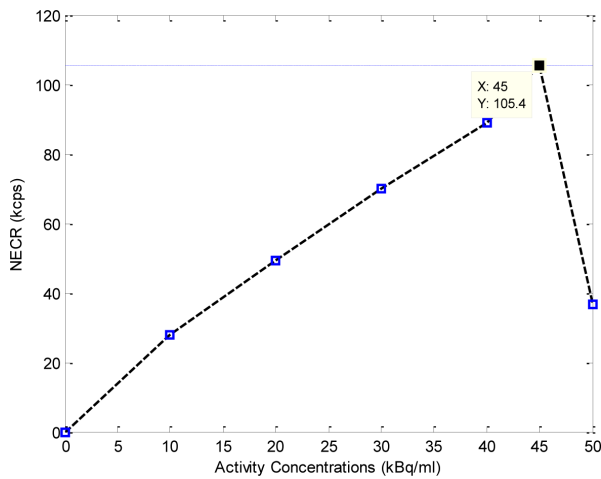
Figure 4: Noise equivalent count rate (NECR) (kcps) for 4 ns timing window and energy window of 350-650 keV with Fludeoxyglucose (F-FDG or FDG), line source for the rat phantom in different activity concentrations (kBq/ml).
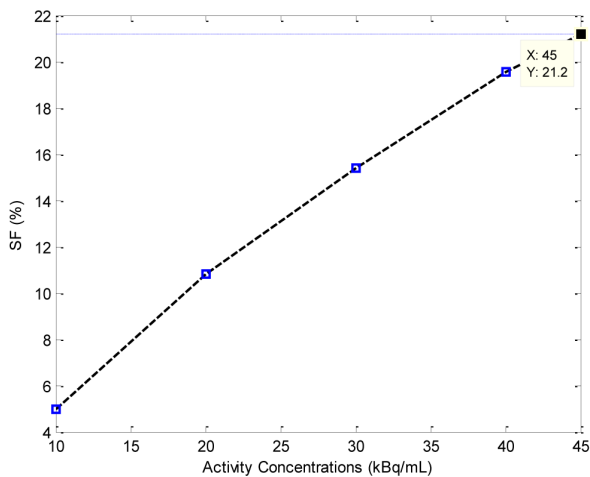

Figure 5: Scatter Fraction (%) for different activity concentrations with an energy window of 350-650 keV and timing window of 4 ns.

detector with an optimized size of axial FOV is proposed with simulations by using Equations 1 and 2 that the best scanner has the maximum sensitivity and minimum number of the crystals and length of axial. Based on Figure 3, the plot peaks at 10.17 cm, and this size is the best for axial FOV because maximum sensitivity was reached, as an important parameter. Also, based on Figure 4, NECR has the most value in this size and the scatter fraction is 21.2% that has less value compared to other systems. In Table 2, comparison of parameters for new design detector and other common detectors were provided. Besides, it is obvious that the new size for the scanner has good ability compared to other scanners.

Conclusion

The new detector was simulated in GATE based on NU 4 in 2008, which has an optimized geometry. The best size of axial FOV and repetitions were calculated, resulting in 10.17 cm and 6 repetitions, respectively, leading to high sensitivity and NECR. Furthermore, the scatter fraction was measured 0.212 in the peak of the NECR, which was low and the results illustrated good ability for this system. This scanner has good ability compared with other scanners according to the results. Sensitivity of this system was obtained 4.65% with LYSO crystal in a timing window of 6 ns and with an energy window of 250-750 Kev, which demonstrated good performance in comparison with other systems.

Table 2: Comparison between different positron emission mammographys (PEMs) and designed PEM (using lutetium yttrium orthosilifcate (LYSO) crystal).

PEM	Energy Window (keV)	Axial FOV (cm)	Crystals size (mm³)	Sensitivity (%)
Designed PEM	350-650	10.17	1.6×1.6×15	3.85
Clear PEM [8]	100-700	11	2×2×20	1.87
Inveon [13]	350-650	12.7	1.5×1.5×10	2.8
Mosaic HP [12]	385-665	11.9	2×2×10	1.77
ALBIRA [19]	350-650	40	40×40×10	2

PEM: Positron emission mammography, FOV: Field of View

Authors' Contribution

S. Setayeshi conceived the idea. D. Roshani wrote the text and he was responsible for the practical implementation of the project. S. Setayeshi supervised the implementation of the project. Both authors read, modified, and approved the final version of the manuscript.

Ethical Approval

This is a simulation study that no ethical approval is required.

Conflict of Interest

None

References

1. Satoh Y, Motosugi U, Imai M, Onishi H. Comparison of dedicated breast positron emission tomography and whole-body positron emission tomography/computed tomography images: a common phantom study. *Ann Nucl Med.* 2020;**34**(2):119-27. doi: 10.1007/s12149-019-01422-0. PubMed PMID: 31768819.

2. Berg E, Cherry SR. Innovations in instrumentation for positron emission tomography. *Semin Nucl Med.* 2018;**48**(4):311-31. doi: 10.1053/j.semnuclmed.2018.02.006. PubMed PMID: 29852942. PubMed PMCID: PMC5986096.

3. Walrand S, Hesse M, Jamar F, Lhommel R. The origin and reduction of spurious extrahepatic counts observed in 90Y non-TOF PET imaging post radioembolization. *Phys Med Biol.* 2018;**63**(7):075016. doi: 10.1088/1361-6560/aab4e9. PubMed PMID: 29513273.

4. Mikhaylova E, Tabacchini V, Borghi G, et al. Optimization of an ultralow-dose high-resolution pediatric PET scanner design based on monolithic scintillators with dual-sided digital SiPM readout: a simulation study. *Phys Med Biol.* 2017;**62**(21):8402. doi: 10.1088/1361-6560/aa8eb2. PubMed PMID: 28944759.

5. Niknejad T, Setayeshi S, Tavernier S, et al. Validation of a highly integrated SiPM readout system with a TOF-PET demonstrator. *Journal of Instrumentation.* 2016;**11**(12):P12003. doi: 10.1088/1748-0221/11/12/P12003.

6. Cherry SR, Sorenson JA, Phelps ME. Tomographic reconstruction in nuclear medicine. *Physics in Nuclear Medicine.* 2003;273-97. doi: 10.1016/B978-1-4160-5198-5.00016-2.

7. Saha GB, Gobal B. Basic of PET imaging: physics, chemistry, and regulations. Springer International Publishing; 2016.

8. Lecoq P, Varela J. Clear-PEM, a dedicated PET camera for mammography. *Nuclear Instruments and Methods in Physics Research Section A: Accelerators, Spectrometers, Detectors and Associated Equipment.* 2002;**486**(1-2):1-6. doi: 10.1016/S0168-9002(02)00666-6.

9. MacDonald L, Edwards J, Lewellen T, Haseley D, Rogers J, Kinahan P. Clinical imaging characteristics of the positron emission mammography camera: PEM Flex Solo II. *J Nucl Med.* 2009;**50**(10):1666-75. doi: 10.2967/jnumed.109.064345. PubMed PMID: 19759118. PubMed PMCID: PMC2873041.

10. Vroonland C. Dedicated mini PET system for breast screening: a technologist's perspective. *Eur J Nucl Med Mol Imaging.* 2010;**37**(Suppl 2):S482-5.

11. Li S, Zhang Q, Vuletic I, Xie Z, Yang K, Ren Q. Monte Carlo simulation of Ray-Scan 64 PET system and performance evaluation using GATE toolkit. *Journal of Instrumentation.* 2017;**12**(02):T02001. doi: 10.1088/1748-0221/12/02/T02001.

12. Goertzen AL, Bao Q, Bergeron M, Blankemeyer E, Blinder S, et al. NEMA NU 4-2008 comparison of preclinical PET imaging systems. *J Nucl Med.* 2012;**53**(8):1300-9. doi: 10.2967/jnumed.111.099382. PubMed PMID: 22699999. PubMed PMCID: PMC4128012.

13. Bao Q, Newport D, Chen M, Stout DB, Chatziioannou AF. Performance evaluation of the inveon dedicated PET preclinical tomograph based on the NEMA NU-4 standards. *J Nucl Med.* 2009;**50**(3):401-8. doi: 10.2967/jnumed.108.056374. PubMed PMID:19223424. PubMed PMCID: PMC2803022.

14. Santin G, Strul D, Lazaro D, Simon L, Krieguer M, Martins MV, Breton V, Morel C. GATE: a Geant4-based simulation platform for PET integrating movement and time management. *IEEE Transactions on Nuclear Science.* 2003;**50**(5):1516-21. doi: 10.1109/TNS.2003.817974.

15. Santin G, Staelens S, Taschereau R, Descourt P, et al. Evolution of the GATE project: new results and developments. *Nucl Phys Proc Suppl.* 2007;**172**:101-3. doi: 10.1016/j.nuclphysbps.2007.07.008.

16. Wiggins C, Santos R, Rugglesb A. A feature point identification method for positron emission particle tracking with multiple tracers. *Nuclear Instruments and Methods in Physics Research Section A: Accelerators, Spectrometers, Detectors and Associated Equipment.* 2017;**843**:22-8. doi: 10.1016/j.nima.2016.10.057.

17. Bailey DL, Maisey MN, Townsend DW, Valk PE. Positron emission tomography. London: Springer; 2005. doi: 10.1007/b136169.

18. Kowalski P, Wiślicki W, Raczyński L, et al. Scatter Fraction of the J-PET Tomography Scanner. *Acta Physica Polonica.* 2016;**47**(2):549. doi: 10.5506/APhysPolB.47.549.

19. Balcerzyk M, Kontaxakis G, Delgado M, et al. Initial performance evaluation of a high resolution Albira small animal positron emission tomography scanner with monolithic crystals and depth-of-interaction encoding from a user's perspective. *Measurement Science and Technology.* 2009;**20**(10):104011. doi: 10.1088/0957-0233/20/10/104011.